MR Imaging–Guided Interstitial Photodynamic Laser Therapy for Advanced Head and Neck Tumors

H. Rolf Jäger, Magali N. Taylor, Tamer Theodossy, and Colin Hopper

Summary: Photodynamic therapy (PDT) is a site-specific tumor treatment involving the administration of a photosensitizer activated by the local application of light. In interstitial PDT (IPDT), multiple laser fibers are inserted into the depth of the tumor. Image guidance is essential for accurate, safe, and uniform light delivery. We report a novel technique of IPDT for advanced head and neck tumors involving an open interventional MR system. Initial results are encouraging, with minimal procedural morbidity, successful palliation of symptoms, and prolongation of expected survival time.

The treatment of head and neck cancer continues to pose a major clinical challenge. Approximately 30–40% of patients with head and neck cancer have persistent or recurrent local-regional disease after the completion of definitive treatment, including surgery, radiation therapy and chemotherapy. Furthermore, 5-year survival rates for patients with cancer of the tongue, mouth and pharynx are only 35% (1, 2).

Photodynamic therapy (PDT) is a minimally invasive treatment that involves the interaction of a photosensitizer in tissue with light (3). Activation of the photosensitizer leads to formation of oxygen free radicals, which cause tissue destruction. The depth of the effect depends on the type of photosensitizer used and the wavelength of the light applied. PDT has been used for surface treatment of superficial mucosal and cutaneous malignancies. The treatment of solid tumors requires the delivery of light into the core of tumor, which is not possible with surface illumination. However, this delivery can be achieved by means of imaging-guided placement of laser fibers into the depth of the tumor (4).

We describe the technical aspects and preliminary results of MR imaging–guided fiber placement for palliative interstitial PDT (IPDT) as a salvage treatment for recurrent head and neck cancers.

Received June 30, 2004; accepted after revision January 10, 2005.

From the Departments of Imaging (H.R.J., M.N.T.), and Maxillofacial Surgery (T.T., C.H.), University College Hospital, Institute of Neurology (H.R.J.), University College London, Lysholm Department of Neuroradiology (H.R.J.), The National Hospital for Neurology and Neurosurgery, and the Eastman Dental Institute for Oral Health Care Sciences (T.T., C.H.), London, United Kingdom.

Address reprint results to H. Rolf Jäger, Lysholm Department of Neuroradiology, The National Hospital for Neurology Neurosurgery, 3rd Floor, 8–11 Queen Square, London WC1N 3BG, United Kingdom.

Methods

Subjects

Patients with significant recurrent disease were sequentially recruited over 4 years from the multidisciplinary head and neck cancer clinic of our institution, a tertiary referral center. The Table summarizes the relevant clinical data, including the patients' ages and the histology, location, and volume of their tumors. All patients had received previous treatment with surgery and irradiation, and seven patients received additional chemotherapy. Patients were considered for IPDT if they were deemed unsuitable for further surgery (because of either unresectability or their tumor or comorbidity) or if dose limits for radiation therapy and chemotherapy had been reached. We obtained institutional ethical approval to treat these patients with advanced head and neck cancer by using PDT, and all patients provided informed consent. They were a subset of patients from a multicenter phase IIB study of the use of PDT for advanced head and neck cancer.

The patients presented with recurrence or persistence of their tumor, and the aim of IPDT was the reduction of tumor size and the symptomatic relief of associated pain, pressure effects, breathing and swallowing difficulties, or discharge. All patients underwent pretreatment MR imaging on a 1.5-T system, and tumor recurrence was histologically confirmed. Three patients with substantial residual tumor or tumor regrowth, as shown on follow-up imaging, were offered repeat IPDT (Table).

Preparation with the Photosensitizer

Intravenous *meso*-tetrahydroxyphenyl chlorine 0.15 mg/kg (mTHPC, Foscan; Biolitec Pharmaceuticals Ltd, Edinburgh, Scotland) was used to sensitize patients 4 days before IPDT. After receiving the injection, patients remained in a low-level lighting setting to prevent photosensitive skin reactions. For the first 24 hours, room light was kept below 100 lx (equivalent to a single 60-W lightbulb) and increased by 100 lx on each subsequent day. After 1 week, patients could go outdoors on overcast days, but they were instructed to avoid direct exposure to sunlight for 3 weeks after photosensitization.

MR Imaging–Guided Needle Placement

All procedures were performed by using a 0.2-T system (Magnetom Open Viva Interventional Scanner; Siemens, Erlangen, Germany). Optical fibers for therapeutic light delivery were inserted through needles with a minimum size of 18 gauge. We used 18-gauge MR-compatible needles (MReye; Cook Europe, Bjaeverskov, Denmark) made of a nonferromagnetic nickel-chromium alloy. Using a honeydew melon as the test object, we determined the best pulse sequence for visual-

Clinical data

Patient/ Age (y)	Diagnosis*	Indication for PDT	Tumor Volume (mL)	Treatment of Spheres (n)	Repeat PDT	Survival after First PDT (wk)†
1/53	Neck node metastasis of tongue SCC	Brachial plexus pain	10	4	No	72
2/60	SCC, base of tongue	Pain	33	8	No	72
3/76	Adenoid cystic carcinoma, maxillary antrum	Nasal obstruction, epistaxis	65	16	At 27 and 51 wk	83
4/45	SCC floor of mouth	Aphonia	24	12	No	24
5/39	Spindle cell carcinoma of cheek‡	Pain, debulking	11	6	At 15 wk	60
6/51	SCC of branchial cyst	Swelling, pain	37	12	At 33 and 57 wk	72
7/69	SCC neck node metastasis	Dysphagia	81	16	No	12
8/54	Hemangiopericytoma submandibular area‡	Debulking, dysphagia	106	32	No	16
9/42	Adenoid cystic carcinoma, parotid	Pain, debulking	13	8	No	Alive at 158 wk
10/50	SCC, tongue	Debulking	58	12	No	1§
11/54	SCC, tonsil	Debulking	122	20	No	18
12/68	SCC, tongue	Pain	41	7	No	38
13/61	SCC, external ear	Debulking	65	16	No	66
14/39	Neuroectodermal tumor, face and neck‡	Debulking	177	32	No	8

* SCC = squamous cell carcinoma.

† Although survival in patients with adenoid cystic carcinoma can be prolonged, expected survival for those with recurrent squamous cell carcinoma is about 2 months.

‡ Survival of rarer tumors is difficult to predict.

§ Died from accidental morphine overdose.

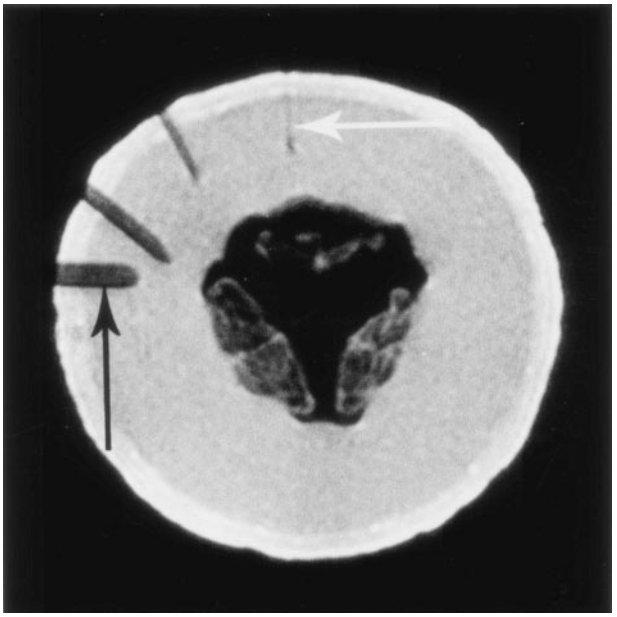

FIG 1. Visualization of the 18-gauge needles by using a 0.2-T interventional magnet, a two-dimensional (2D) fast low-angle shot (FLASH) sequence (TR/TE/NEX = 341/12/1), and a melon as the test object. Magnetic-susceptibility artifact from the needles, which are of identical size, increased with their angle from the *Z* axis. Needle in alignment with the *Z* axis of the magnet (vertical) is barely visible (*white arrow*), but needles at an angle of ≥30° are well demonstrated. Needle perpendicular to the *Z* axis shows the most pronounced susceptibility artifact, with exaggeration of its actual diameter (*black arrow*).

izing these needles and assessed the size of the needle artifact at various orientations to the main magnetic field (Fig 1). We tested the following pulse sequences: T2-weighted turbo spin-echo (SE), sequential-section fast imaging with steady precession (FISP), FISP with balanced gradients in all spatial directions (True-FISP), a time-reversed version of FISP, and 2D and 3D FLASH. The 2D FLASH sequence provided the best visualization of the 18-gauge needles on our 0.2-T system. Imaging parameters were TR/TE/NEX = 341/12/1, FOV = 219 × 350 mm, matrix = 122 × 256, multislice acquisitions, 6-mm-thick sections without a gap, 11 sections, and 44-second acquisition time. The image update time in the in-room monitor was about 30 seconds. The needles could be identified without problems if they were inserted at an angle of more than 30° with respect to the main magnetic field B_0 (*Z* axis). They were only faintly visible when they were aligned with the *Z* axis of the magnet (Fig 1).

Most patients received a general anesthetic by using MR-compatible equipment, but four procedures were performed with the patients under local anesthesia. Preliminary MR images were acquired after the placement of lipid capsules (primrose oil; Boots Healthcare International, UK) on the skin overlying the target area to provide high-signal-intensity surface landmarks for planning of the skin-entry sites. The best possible needle trajectory was determined on images acquired in multiple planes. The anatomic access route to the tumor was dictated by bony structures, around which the needles had to be negotiated; by vital structures, which had to be avoided; and by the anticipated angle of the needles with respect to the *Z* axis, which could be altered by changing the position of the patient's head.

The 18-gauge needles (MReye; Cook Europe) were available in lengths of 5, 10, or 15 cm. The number and length of the needles was determined by the size and orientation of the tumor. Using MR imaging guidance, we advanced the needles into the deepest treatable part of the tumor, taking care to maintain an adequate distance from the major blood vessels.

Detailed technical aspects of needle positioning for laser light delivery are outlined in the illustrative cases described later.

Laser Treatment

A diode laser (Diomed Ltd., Cambridge, UK or Ceramoptec GmbH, Bonn, Germany) with a wavelength of 652 nm was used as the light source. The primary beam was fed into a beam splitter to produce four treatment fibers with a core diameter

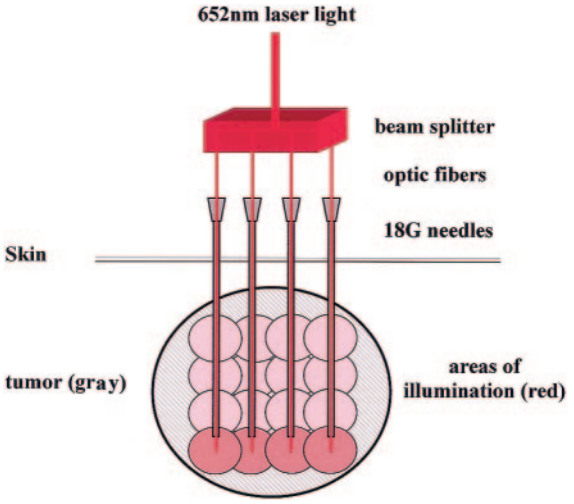

FIG 2. Schematic of IPDT. Primary laser beam (652-nm wavelength) is split into four treatment fibers, which allow for simultaneous delivery of light at four points. Optic fibers are fed through 18-gauge needles placed under MR imaging guidance; they protrude slightly beyond the needle tips. Energy deposition of 20 J via these fibers illuminates an area of about 10 mm in radius, in which the photosensitizer is activated. Deepest parts of the tumor are illuminated first (*red spheres*). Subsequent incremental withdrawal of the laser fibers and needles with further energy deposition produces overlapping spheres of illumination (*pink*), leading to activation of photosensitizer in the most of the tumor.

of 0.4 mm and power of 100 mW (Fig 2). The optical fibers were passed down the 18-gauge needles to leave 1 mm of bare fiber in direct contact with tumor tissue during light delivery. The energy applied through each fiber was 20 J, which was sufficient to activate the photosensitizer in a radius of approximately 10 mm in the soft tissue. After the deepest portion of the tumor was treated, the needles and laser fibers were pulled back in 1-cm increments. Each withdrawal was followed by further illuminations of 20 J until the maximum amount of the tumor was treated (Fig 2). Depending on the depth and complexity of treatment, MR imaging–guided needle placement took 20–40 minutes. Each set of four treatment locations was illuminated for 200 seconds, and total illumination times were 200–1600 seconds, depending on the size of the tumor.

Results

Early treatment effects were assessed with MR imaging 4–8 days after IPDT. Contrast-enhanced T1-weighted images showed areas of tumor necrosis in all patients, with the exception of the patient with a spindle cell carcinoma of the cheek, which was a poorly enhancing tumor. Areas of necrosis became confluent where the spheres of illuminated tissue overlapped, either from parallel fibers or along the longitudinal axis of an individual fiber track. When measured in a perpendicular direction to a fiber track, the extent of tissue damage corresponded to a radius of 9–11 mm (Fig 3).

Seven patients underwent follow-up MR imaging at 1–3 months. Images showed tumor shrinkage or stable tumor size. In one patient, who was still alive at last follow-up, images showed persistent shrinkage of the tumor at 7 months after treatment. Three patients were offered repeat IPDT (4, 7, and 8 months after initial IPDT) after MR imaging showed significant residual tumor or tumor recurrence. In two, IPDT was repeated at 12 and 14 months after initial treatment (Table).

All patients experienced relief of symptoms after IPDT. Survival of all but two patients exceeded the expected prognosis of recurrent head and neck tumors, which is approximately 2 months for recurrent SCC. One patient died from an accidental morphine overdose at 1 week, and another patient with an exceptionally large tumor died 8 weeks after IPDT. Overall survival was worse if the tumor volume exceeded 100 cm^3 than if it did not (Table).

Illustrative Cases

Case 1.—The patient was a 61-year-old man with an SCC of the external auditory meatus extending along the soft tissues of his left cheek (Fig 3). The entire tumor was treated by using the four fibers inserted in a posteroanterior direction. Care was taken to avoid the proximal petrous portion of the carotid artery. Adequate visualization of the 18-gauge needles was achieved by rotating patient's head to the right, resulting in a 45° angle between the needles and the *Z* axis. The distribution of the needles in the tumor was verified in three planes before we commenced with the application of laser light. Necrosis of more than 90% of the tumor was achieved, and the patient survived 16.5 months after treatment.

Case 2.—The patient was a 54-year-old man with a large, recurrent hemangiopericytoma of the base of the tongue, which was treated by using a submental approach (Fig 4). Images obtained in the plane of the needle shafts proved particularly useful for correcting the entry angle and for ensuring a parallel course of the needles. After their initial insertion, the needles were too close to the mandible. They were easily redirected toward the core of the tumor with the aid of sagittal MR images. The patient survived 4 months after IPDT.

Case 3.—The patient was a 51-year-old woman with a recurrent branchial duct carcinoma who received surgery, radiation therapy, and chemotherapy (Fig 5). The tumor was intimately related to the left internal carotid artery. A lateral approach was used, and visualization of the needle tips on MR imaging was crucial for maintaining the minimal required distance from the artery to avoid carotid blowout. A large part of the tumor showed subsequent necrosis, including areas close to the internal carotid artery, which was preserved. This patient received further IPDT after 8 and 14 months and survived for 18 months after initial IPDT with a good quality of life.

Case 4.— The patient was a 76-year-old man with a recurrent adenocarcinoma of the right maxillary antrum who had previous surgery, including enucleation of the right eye, as well as chemotherapy and radiation therapy (Fig 6). He complained of persistent nasal obstruction and bleeding. Eighteen-gauge needles were inserted in an anteroposterior direction, and the patient's head was tilted 30° degree to left to

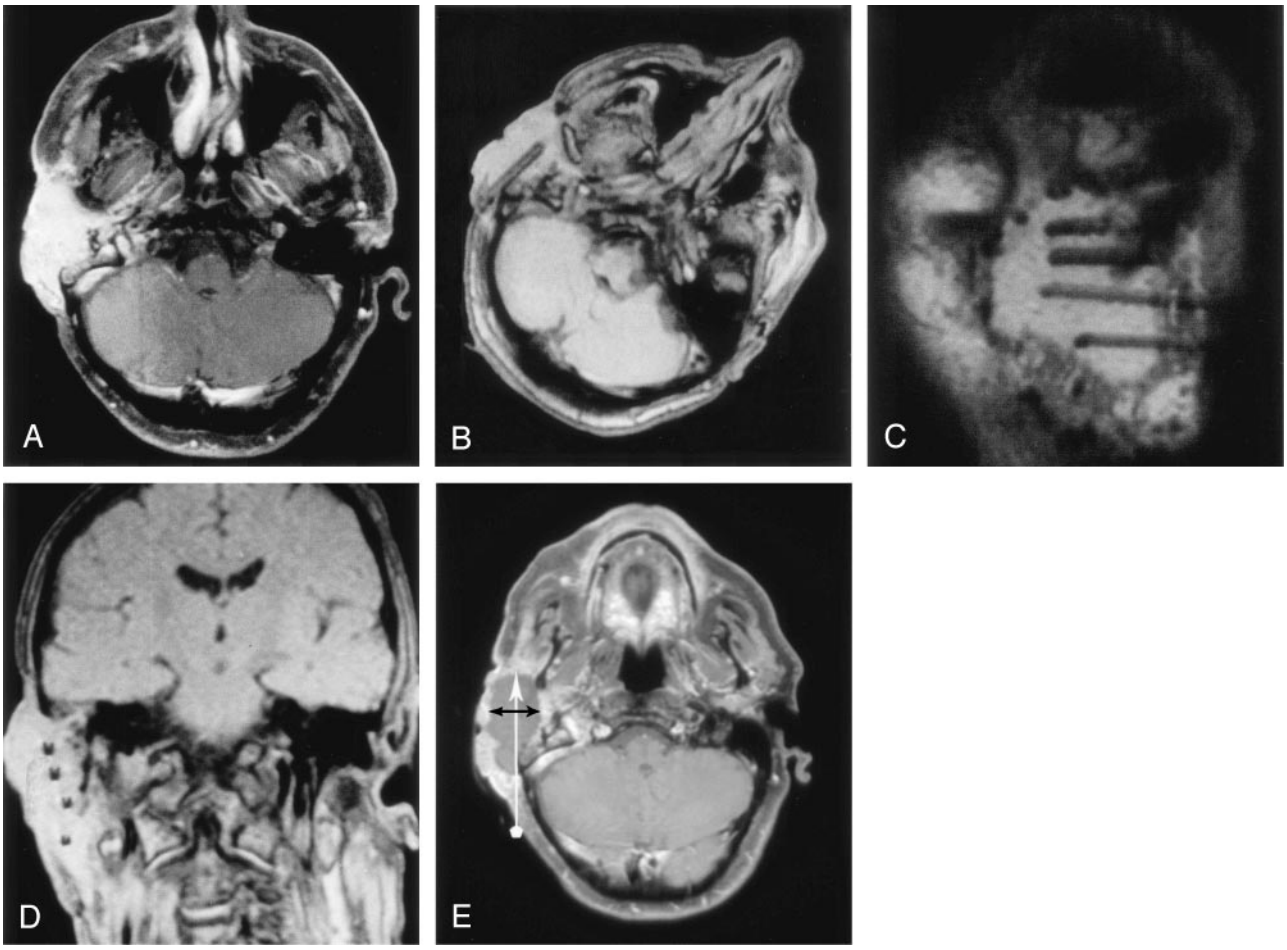

FIG 3. IPDT of an SCC arising from the external auditory meatus.

A, Axial enhanced T1-weighted SE image (TR/TE/NEX = 893/15/2) obtained 3 days before IPDT shows a strongly and relatively homogenously enhancing tumor.

B–D, Axial (*B*), oblique sagittal (*C*), and oblique coronal (*D*) 2D FLASH images (TR/TE/NEX = 341/12/1) obtained during treatment show an approximately equal distribution of four 18-gauge needles in the tumor. Rotation of the patient's head, as shown in *A,* avoids alignment of the needles with the *Z* axis and increases their visibility.

E, Axial enhanced T1-weighted SE image obtained 6 days after treatment shows an extensive nonenhancing area of tumor necrosis. *Vertical arrow* shows the needle trajectory during IPDT. *Horizontal arrows* indicates the diameter of the area of necrosis perpendicular to the needle trajectory.

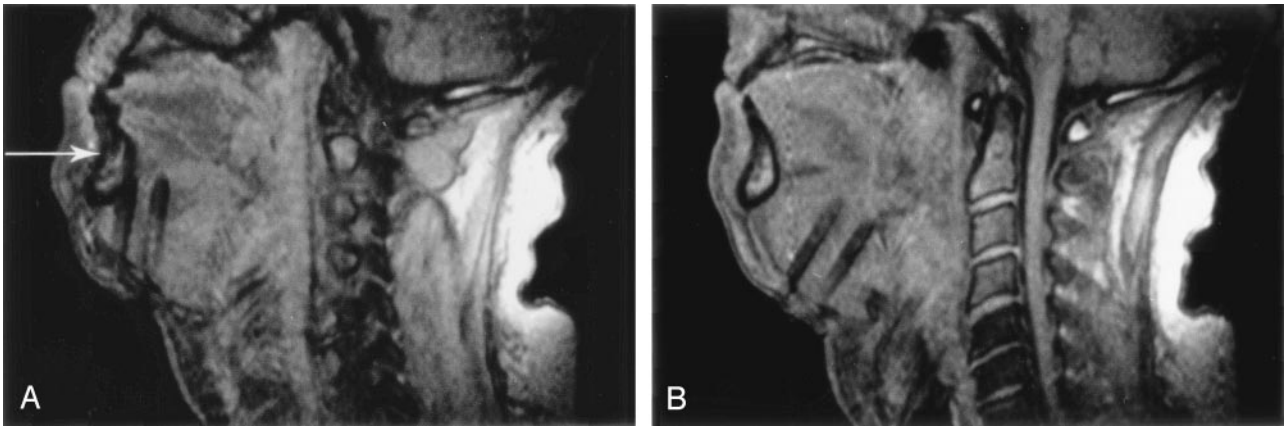

FIG 4. Sagittal 2D FLASH images obtained during IPDT of a hemangiopericytoma at the base of the tongue.

A, Initial entry angle of the 18-gauge needles, based on palpation of the tumor, had been misjudged, and the needles came to lie close behind the mandible (*arrow*). Needle artifact is large because of the almost-90° angle with the *Z* axis.

B, Imaging in the plane of the needle shafts allowed for easy correction of the entry angle and redirection of the needles toward the center of the tumor.

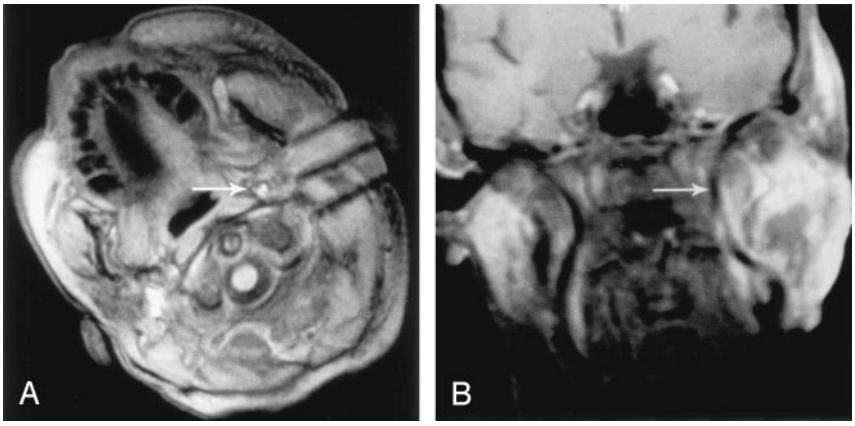

FIG 5. IPDT of a branchial duct carcinoma.

A, 2D FLASH image shows the position of the needles in the tumor before insertion of the laser fibers. Middle needle points toward the left internal carotid artery (*arrow*), which is hyperintense because of inflow effects. Distance of at least 15 mm from the vessel must be maintained to avoid carotid blowout.

B, Coronal enhanced T1-weighted SE image at 5 days after treatment shows areas of necrosis in the tumor and preservation of the internal carotid artery (*arrow*), which is hypointense because of flow void.

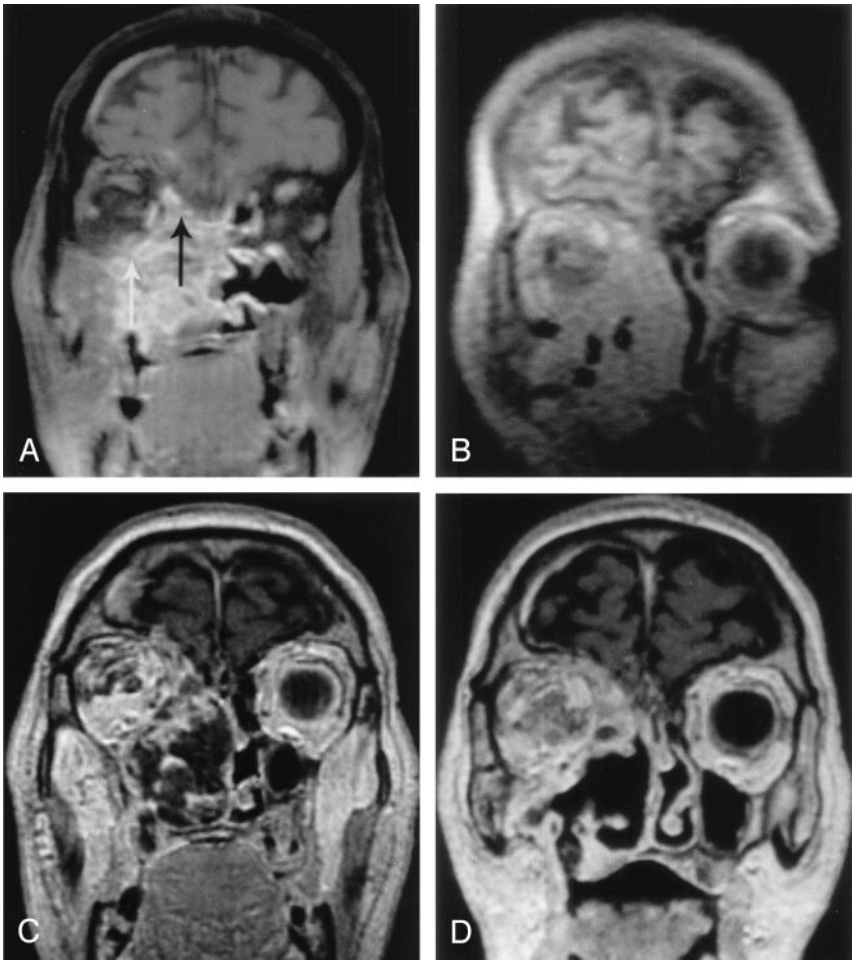

FIG 6. IPDT of a recurrent adenoid cystic carcinoma of the right maxillary antrum.

A, Coronal enhanced T1-weighted SE image before treatment shows the extensive, enhancing tumor invading neighboring structures, including the extraconal space of the right orbit (*white arrow*) and the floor of anterior cranial fossa (*black arrow*).

B, Coronal oblique 2D FLASH image shows the position of the 18-gauge needles in the tumor mass.

C, Coronal enhanced T1-weighted SE image at 5 days after treatment shows markedly reduced tumoral enhancement with areas of necrosis.

D, Coronal enhanced T1-weighted SE image at 6 weeks after treatment shows that a substantial portion of the necrotic tumor has sloughed off.

avoid alignment of the needles with the *Z* axis. IPDT resulted in necrosis of the bulk of the tumor, which subsequently sloughed off. The patient no longer complained of nasal discharge. He underwent repeat IPDT after 4 and 12 months and survived 21 months after initial treatment.

Discussion

The prognosis for patients with head and neck tumors remains poor, and treatment continues to be a major clinical challenge. Although some early cancers can be cured, as many as 40% of patients have persistence or recurrence of their disease after definitive treatment, which usually consists of a combination of surgery and radiation therapy. Salvage surgery is technically difficult; it may be disfiguring; and it carries a high risk of complications, including damage to neurovascular structures (1). Further radiation therapy is often not possible because the surrounding tissue may have already received a maximal tolerable dose of ionizing radiation, and conventional chemotherapy has a disappointing response rate (5).

Two forms of medical laser therapy are available:

thermal laser therapy and photodynamic laser therapy (3). The former uses heat to achieve tissue destruction, and the latter is based on the interaction of a photosensitizing agent, light of a specific wavelength matched to the absorption peak of the drug, and oxygen. In PDT tissue temperature does not increase, and the cytotoxic effect is due to the formation of reactive singlet oxygen, which occurs after activation of the photosensitizer by light. At the periphery of the treated site, no necrosis occurs when the light energy falls below a threshold level. In addition to being cytotoxic, PDT also causes damage to the microvasculature. This damage contributes to tumor destruction and is responsible for tissue swelling in the first few days after PDT. The structural integrity of normal connective tissue, such as collagen and elastin, is well preserved after PDT, in contrast to thermal laser therapy (3, 4).

Because penetration of light in the tissue is limited, PDT was initially used for the treatment of superficial lesions of the skin and hollow organs (3, 4), including premalignant and malignant conditions of the oral cavity (6). Good results have been obtained with endoscopic treatment of small cancers of the major airways, esophagus, stomach, and colon (3, 4).

Treatment of solid tumors requires IPDT, in which light is delivered into the depth of the tumor. IPDT has been used to treat inoperable cancer of the pancreas by using CT or sonographic guidance (7) and recurrent prostate cancer after radiation therapy by using transrectal sonographic or MR guidance (8). Study results are encouraging and show that substantial necrosis of solid tumors can be achieved with imaging-guided light delivery.

Correct intratumoral placement of MR-compatible needles, which can accommodate laser fibers, is crucial for this technique. MR-compatible needles are nonferromagnetic alloys and generate a susceptibility artifact at their interface with tissue; this artifact consists mostly of signal intensity loss with little or no geometric distortion. The size and visibility of this artifact depends on a number of factors, including the magnetic field strength, the orientation of the needle to the main magnetic field B_0 (Z axis), the pulse sequence used, the section thickness, and the diameter and composition of the needle (9). At a given magnetic filed strength, the angle of the needle shaft relative to B_0 is the most important factor, with greater angles causing larger artifacts. The needles we used were made of a nonferromagnetic nickel-chromium alloy with high nickel and low iron content, which created an artifact slightly larger than that of titanium-alloy needles.

Our experiment with a melon as the test object showed that the 2D FLASH sequence was best for demonstrating the 18-gauge needles. The visibility of the needles was noticeably superior with the 2D FLASH sequence than with the FISP or true FISP sequences, which other investigators used (10, 11). In addition, the FISP sequences increased the number of distortion artifacts at the periphery of our test object. Therefore, we chose the 2D FLASH sequence despite its longer image acquisition and recall times, which precluded real-time imaging of the needle placement. We found that image availability between 1 and 2 minutes after needle placement was clinically acceptable.

Needles in line with the Z axis were only faintly visible and too unreliable to detect in heterogeneous tumor tissue. An angulation of 30° or more enabled consistent identification of the needle position in all of our clinical cases. The low-field-strength system we used had a vertical field C-shaped magnet with the Z axis perpendicular to the patient in a supine position. Therefore, needles inserted in an inferosuperior direction, as in a submental approach for a tumor at the base of the tongue generated the largest needle artifact (Fig 4). Conversely, in tumors requiring an anteroposterior or posteroanterior approach, the needles would have been difficult to detect if the patient's head position were straight. In such cases, rotation of the patient's head by at least 30° ensured adequate visualization of the needles (Fig 3). Most low-field magnets have a similar design with two horizontal magnetic poles and a Z axis vertically aligned relative to the patient (8); therefore, these positioning techniques apply. However, all high-field and most mid-field scanners have a different design, with a tube-shaped magnet and the Z axis running along the patient's head-to-feet direction. Therefore, different positioning rules apply to such systems, and other maneuvers, such head extension, may be needed to increase the angle with the Z axis when a horizontal needle trajectory is required. A higher-field-strength magnet may also require a different pulse sequence to generate less artifact for needle localization.

Image guidance for IPDT is essential to avoid damage to vital structures and to ensure homogenous light delivery to the tumor. Both of these objectives are difficult to achieve with blind needle insertion based on palpation only. One patient who was treated in the early phase of IPDT for recurrent neck disease without image guidance died from carotid blowout 2 weeks after treatment. Postmortem examination showed probable tumoral invasion of the artery; therefore, the damage was likely caused by treatment of tumor invading the carotid wall. With MR imaging–guided IPDT, one can ensure that light is delivered at a safe distance from the neck arteries. With the predicated radius of light diffusion in tissue being approximately 10 mm (4), we observed a minimum distance of 15 mm between the 18-gauge needles and the major arteries (Fig 4). Using this technique, we have been able to treat tumors close to neck arteries without the complication of an arterial blowout.

Homogeneous delivery of light to the tumor is important to maximize tissue destruction. Analogous to the Paris system for brachytherapy, which dictates that radioactive sources should be parallel, be equidistant, and have a constant activity along the radioactive source (12), optic fibers in IPDT should lie parallel to each other and be separated by 1.5–2 cm to ensure an overlap of treatment spheres. In the initial phase of IPDT, we used sonographic and CT guidance, although sonography is restricted by bony struc-

tures of the head and neck, which impede the penetration of sound. Cross-sectional CT is limited to the axial plane and makes it more difficult to image and correct oblique needle trajectories, which are often necessary because of the complex anatomy in the head and neck.

Multiplanar MR imaging can be adapted to the patient's anatomy and facilitates equidistant placement of the needles in the tumor. Images acquired in the plane of the needle path are particularly useful for correcting the entry angle of the needles, which can easily be misjudged (Fig 4). This feature is important because multiple needles should have similar entry angles to avoid convergence or divergence of their tips in the depth of the tumor.

MR imaging-guided IPDT produces areas of necrosis in head and neck tumors, which appear as regions of nonenhancing regions on early postprocedural MR images. Enhancing tissue surrounding the necrotic areas could represent an inflammatory reaction or a rim of residual tumor. The extent of tumor destruction achieved was in concordance with the imaging findings described after IPDT of pancreatic and prostate cancer (7, 8). In pancreatic carcinomas, IPDT induced a necrosis with a typical radius of 9 mm (range, 7–11 mm) on enhanced CT scans obtained a few days after treatment (7). IPDT of prostate cancer produced prostatic necrosis of up to 91% on follow-up MR imaging; this was accompanied with a substantial decrease in prostate-specific antigen levels in most patients (8).

The patients treated with MR imaging–guided IPDT had relief from pressure effects, nasal discharge, and pain. Most survived beyond the predicted life expectancy of patients with recurrent head and neck tumors (about 2 months for those with recurrent SCC and a little longer for those with adenoid cystic carcinoma) without further treatment. A clinical study was conducted of all head and neck tumors treated with IPDT at our institution, including those initial patients treated with blind needle insertions and those treated under CT and US guidance. The results showed an overall response rate of 89% with a local control rate of 54% and 41% at 6 and 12 months, respectively, with a median life expectancy of 15 months (13).

MR imaging–guided IPDT must be viewed in the context of other imaging-guided tumor-ablation therapies, including cryosurgery, radio-frequency lesion ablation, laser interstitial thermal therapy (10–11, 14–16). All of these methods use alteration of tissue temperature to achieve tumor necrosis. The principle of cryosurgery is in situ freezing and tumor destruction by means of ice crystal formation, whereas radio-frequency ablation and laser interstitial thermal therapy cause localized tissue heating, resulting in coagulative necrosis. All of these ablative therapies have been used for the treatment of primary and secondary liver tumors (14). Percutaneous MR imaging–guided radio-frequency ablation of the tongue base has been evaluated in clinical studies to develop a new treatment for sleep apnea (15) and in porcine models (16). Laser interstitial thermal therapy has been used to treat recurrent head and neck tumors (10, 11). Unlike us, previous authors used CT-guided placement of a laser application system consisting of a 9F sheath, a 7F thermostable protective catheter, and a laser applicator. MR imaging with thermosensitive T1-weighted gradient-echo sequences was then used to monitor temperature changes in tumor tissue during laser treatment. Signal intensity loss due to heat started 3 minutes after laser irradiation and rapidly progressed to cover a maximal diameter of 26 mm. In one case, the investigators had to interrupt the treatment because of a rapid extension of this zone toward the internal carotid artery (10).

IPDT of head and neck tumors appears to offer several advantages compared with the ablation techniques just described. First, IPDT causes no thermal effect, and damage to healthy connective tissue, muscles and nerves is limited. This feature allows for the treatment of subcutaneous tumors close to the surface without causing skin necrosis. Animal studies on the sciatic nerves in mice (17) showed that nerve tissue is relatively resilient to PDT. None of our patients developed new cranial nerve palsies after IPDT despite the proximity of the facial and hypoglossal nerves to the treated area in some. Second, evidence suggests that the photosensitizer we used preferentially accumulates in tumor tissue (4), which makes IPDT a treatment more specific to tumor tissue than the thermal methods. Third, intraprocedural monitoring of temperature changes to control the extent of tissue damage is not needed. Compared with laser interstitial thermal therapy, IPDT creates a relatively small and well-defined radius of tumor destruction around a fiber tip. The use of multiple needles and small, overlapping treatment spheres, as described herein, allows for more-tailored tissue destruction, which can be adapted to asymmetrical tumor boundaries. With laser interstitial thermal therapy, tissue destruction is governed by the concentric spread of temperature changes around the single laser applicator.

The adverse effects of IPDT are transient local edema and increased light sensitivity. Local edema can cause temporary swelling around the treated area, which may cause some discomfort, but this usually subsides after 1 or 2 weeks. Light sensitivity after administration of the photosensitizer can lead to skin burns if the necessary precautions are not taken. Low-level lighting is particularly important during the first few days, and if patients must be exposed to more intense light, they should wear dark glasses and cover all areas of their skin. Major complications, such as carotid a blowout, did not occur with MR imaging–guided IPDT.

IPDT can be used after previous surgery, radiation therapy, or chemotherapy. One of its biggest advantages is the lack of cumulative toxicity. Although repeated use of radiation therapy and chemotherapy is limited, IPDT can be applied many times at the same site, given a minimum interval of 6 weeks between treatments to allow the surrounding tissue to recover.

Conclusion

IPDT is a promising new form of salvage treatment for advanced head and neck tumors. Its response rates are on a par with if not better than those of other local-regional treatments. It provides better cosmetic outcomes and less functional morbidity than repeat surgery or radiation therapy. The use of MR guidance, as we describe, increases the safety and efficacy of IPDT. It allows for treatment of a maximum proportion of the tumor while minimizing the risk of complications related to damage of the underlying structures.

Acknowledgments

The authors would like to acknowledge A. D. Priest, Department of Medical Physics and Bioengineering, University College Hospitals Trust, London, United Kingdom, for his help in optimizing the MR parameters for needle visualization on the 0.2-T interventional magnet and Sandy Mosse, Department of Medical Physics and Bioengineering, University College Hospitals Trust, London, United Kingdom, for his technical assistance during the IPDT treatments.

References

1. Watson JC, Ridge JA. **Surgical management of local and regional recurrent head and neck squamous cell carcinoma.** *Curr Opin Oncol* 1998;10(3):207–212
2. Sant M for the Eurocar working group. **Overview of EUROCAR-2 results on survival of cancer patients diagnosed in 1985–1989.** In: Berrino F, Capocaccia R, Esteve J, et al, eds. *Survival of Cancer Patients in Europe: The EUROCARE-2 Study*. IARC Scientific Publication No 151. Lyon, France: IARC; 1999:525–543
3. Bown SG. **Science, medicine, and the future: new techniques in laser therapy.** *BMJ* 1998;316(7133):754–757
4. Hopper C. **Photodynamic therapy: a clinical reality in the treatment of cancer.** *Lancet Oncol* 2000;1:212–219
5. Stewart FA. **Re-treatment after full-course radiotherapy: is it a viable option?** *Acta Oncol* 1999;38(7):855–862
6. Hopper C, Kubler A, Lewis H, Tan IB, Putnam G. **mTHPC-mediated photodynamic therapy for early oral squamous cell carcinoma.** *Int J Cancer* 2004;111(1):138–146
7. Bown SG, Rogowska AZ, Whitelaw DE, et al. **Photodynamic therapy for cancer of the pancreas.** *Gut* 2002;50(4):549–557
8. Nathan TR, Whitelaw DE, Chang SC, et al. **Photodynamic therapy for prostate cancer recurrence after radiotherapy: a phase I study.** *J Urol* 2002;168:1427–1432
9. Frahm C, Gehl HB. **Passive visualization strategies for biopsy and needle puncture.** In: Lufkin RB, ed. *Interventional MRI.* St Louis: Mosby; 1999:130–136
10. Vogl TJ, Mack MG, Muller P, et al. **Recurrent nasopharyngeal tumors: preliminary clinical results with interventional MR imaging–controlled laser-induced thermotherapy.** *Radiology* 1995;196(3):725–533
11. Mack MG, Vogl TJ. **MR-guided ablation of head and neck tumors.** *Neuroimaging Clin N Am* 2004;14(4):853–859
12. Dutreix A and Marinelo G. **The Paris system.** In: Pierquin B, Wilson JF, Chassagne D, eds. *Modern Brachytherapy*. New York: Masson; 1987:25–42
13. Lou PJ, Jager HR, Jones L, Theodossy T, Bown SG, Hopper C. **Interstitial photodynamic therapy as salvage treatment for recurrent head and neck cancer.** *Br J Cancer* 2004;91(3):441–446
14. Dick EA, Taylor-Robinson SD, Thomas HC, Gedroyc WM. **Ablative therapy for liver tumours.** *Gut* 2002;50(5):733–739
15. Stuck BA, Starzak K, Hein G, Verse T, Hormann K, Maurer JT. **Combined radiofrequency surgery of the tongue base and soft palate in obstructive sleep apnoea.** *Acta Otolaryngol* 2004;124(7):827–832
16. Nour SG, Lewin JS, Gutman M, et al. **Percutaneous MR imaging-guided radiofrequency interstitial thermal ablation of tongue base in porcine models: implications for obstructive sleep apnea syndrome.** *Radiology* 2004;230(2):359–368
17. Christensen NR, Charabi S, Johansen LS, et al. **Effect of photodynamic therapy on a heterotransplanted human parotid tumor.** *Auris Nasus Larynx* 2000;27(3):241–245